Experimental study of cesium $5D + 5D \rightarrow 6S + (nL = 9D, 11S, 7F)$ energy pooling collisions

Qian Wang (王 倩)[1,2], Kang Dai (戴 康)[2], and Yifan Shen (沈异凡)[2]

[1] *School of Science, Xi'an Jiaotong University, Xi'an 710049*

[2] *Department of Physics, Xinjiang University, Urumqi 830046*

Received November 13, 2006

We report experimentally the measured rate coefficients for the energy pooling (EP) collisions process $\mathrm{Cs}(5D)+\mathrm{Cs}(5D) \rightarrow \mathrm{Cs}(6S)+\mathrm{Cs}(nL = 9D, 11S, 7F)$ in cesium densities of $10^{16}-10^{17}$ cm^{-3} . The $5D$ state was populated via $8S \rightarrow 7P \rightarrow 5D$ spontaneous emission following two-step pumping $6S \rightarrow 6P_{3/2} \rightarrow 8S$. Since the $5D \rightarrow 6P$ (3.0—3.6 μm) fluorescence could not be detected in this experiment, we carried out a relative measurement for the process $6P + 5D \rightarrow 6S + 7D$. The excited-atom density and spatial distribution were mapped by monitoring the absorption of a counterpropagating single-mode laser beam, tuned to $6P_{3/2} \rightarrow 9S_{1/2}$ transition, which could be translated parallelly to the pump beam. The excited atom densities have been combined with the measured fluorescence ratios to yield EP rate coefficients. The average values for $nL = 9D, 11S$ and $7F$ are 8.0 ± 4.0, 7.0 ± 3.5, and 9.3 ± 4.6 (in units of 10^{-10} cm^3/s), respectively. Influence of the energy transfer process $11S + 6S \leftrightarrow 7F + 6S$ on the rate coefficients k_{11S} and k_{7F} is also discussed.

OCIS codes: 020.0020, 020.2070.

Energy pooling (EP) collision is a process where two excited atoms collide and produce one highly excited atom and one ground-state atom[1]. Typically optical excitation is used to prepare the colliding partners in the excited state, and the highly excited atoms, populated by the EP collisions, are detected through their fluorescence. The process has been extensively studied in alkali-metal vapors for both homonuclear[2,3] and heteronuclear systems[4], as well as in other metal vapors[5]. Measurements of EP rate coefficients at thermal energies provide information on atom-atom interactions at large interatomic distances, which are of particular interest in the new field of ultracold atom collisions. While the majority of previous alkali-metal work has concentrated on the EP collisions between two alkali atoms excited to the first resonance level[3,6] , there has been little work on the EP collisions between two highly excited atoms. Here we report experimental rate coefficients for the EP collisions:

$$\mathrm{Cs}(5D) + \mathrm{Cs}(5D) \xrightarrow{k_{nL}} \mathrm{Cs}(6S) + \mathrm{Cs}(nL = 9D, 11S, 7F), \tag{1}$$

where k_{nL} indicates the EP rate coefficient.

In the experiment the cesium atoms are excited to the $8S$ state using two single-mode diode lasers in two steps. When the cesium atoms densities are more than 10^{16} cm^{-3}, higher-lying levels of cesium atoms are populated by the EP collisions because of the increase of radiation trapping[7] (see Fig. 1). The $5D$ level is populated via $8S \rightarrow 7P \rightarrow 5D$ spontaneous emission. To determine rate coefficients for the EP collisions, we have to measure the fluorescence intensity from the $5D$ state as well as the cesium atom density in the $5D$ state. Because the fluorescence of $5D \rightarrow 6P$ transition (3.0—3.6 μm) is in the infrared and can not be detected in this experiment, we carry out a relative measurement to the following process[8],

$$\mathrm{Cs}(6P) + \mathrm{Cs}(5D) \xrightarrow{k_{7D}} \mathrm{Cs}(7D) + \mathrm{Cs}(6S). \tag{2}$$

The rate coefficients k_{nL} of the process (1) can be obtained by measurement of the fluorescence ratio I_{nL}/I_{7D} $(nL = 6P, 9D, 11S, 7F)$ and the atom density in the $6P$ state.

In the experiment we have also established the contribution of the energy transfer process

$$\mathrm{Cs}(11S) + \mathrm{Cs}(6S) \underset{k_2}{\overset{k_1}{\longleftrightarrow}} \mathrm{Cs}(6S) + \mathrm{Cs}(7F). \tag{3}$$

Process (3) is expected to be strong since the $11S$ and $7F$ levels lie very close in energy ($\Delta E = 18$ cm^{-1}).

The steady-state rate equations for the population in state nL $(nL = 9D, 11S, 7F)$ read

$$\frac{\mathrm{d}n_{9D}}{\mathrm{d}t} = 0 = \frac{1}{2}k_{9D}n_{5D}^2 - \Gamma_{9D}n_{9D}, \tag{4}$$

$$\frac{\mathrm{d}n_{11S}}{\mathrm{d}t} = 0 = \frac{1}{2}k_{11S}n_{5D}^2 + k_2 n n_{7F} - k_1 n n_{11S} - \Gamma_{11S}n_{11S}, \tag{5}$$

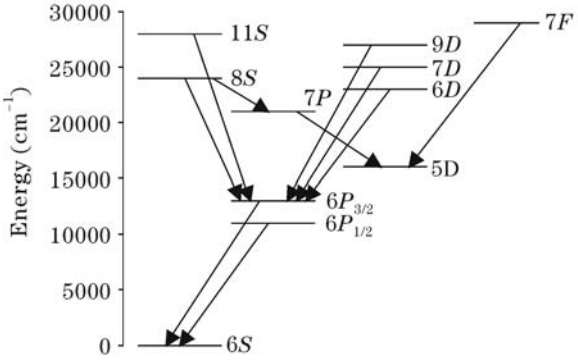

Fig. 1. Energy levels of cesium transitions.

$$\frac{\mathrm{d}n_{7F}}{\mathrm{d}t} = 0 = \frac{1}{2}k_{7F}n_{5D}^2 + k_1 n n_{11S} - k_2 n n_{7F} - \Gamma_{7F}n_{7F}. \tag{6}$$

For process (2), the steady-state rate equation for the population in state $7D$ reads

$$\frac{\mathrm{d}n_{7D}}{\mathrm{d}t} = 0 = k_{7D}n_{6P}n_{5D} - \Gamma_{7D}n_{7D}, \tag{7}$$

here n is the density of ground state atoms, n_{nL} is the density in the atomic level nL, Γ_{nL} is the total radiative rate from level nL, k_1 and k_2 are the rate coefficients of process (3) in the two directions, which connected by the detailed balance principle involving the level degeneracy as

$$\frac{k_1}{k_2} = \frac{g(7F)}{g(11S)}\exp\left(-\frac{\Delta E}{kT}\right). \tag{8}$$

In our experiment, $k_1/k_2 \approx 6.7$. From Eqs. (5) and (6), the relation for the population of the $7F$ and $11S$ levels is given by

$$\frac{n_{7F}}{n_{11S}} = \frac{k_{7F}k_1 n + k_{7F}\Gamma_{11S} + k_{11S}k_1 n}{\Gamma_{7F}k_{11S} + k_{7F}k_2 n + k_{11S}k_2 n}. \tag{9}$$

From Eqs. (4) and (5), the rate coefficient k_{11S} is given by

$$k_{11S} = \frac{[\Gamma_{11S} + k_1 n - k_2 n(n_{7F}/n_{11S})]k_{9D}}{\Gamma_{9D}(n_{9D}/n_{11S})}, \tag{10}$$

k_{9D} can be obtained from Eqs. (4) and (7) as

$$k_{9D} = 2k_{7D}^2\frac{\Gamma_{9D}}{\Gamma_{7D}^2}\frac{n_{9D}}{n_{7D}}\frac{n_{6P}}{n_{7D}}n_{6P}. \tag{11}$$

The population ratios in Eqs. (9)—(11) are given by the relevant intensity ratios

$$\frac{I_{nL\to n''L''}}{I_{n'L\to n''L''}} = \frac{h\nu_{nL}}{h\nu_{n'L'}}\frac{\varepsilon_{nL}}{\varepsilon_{n'L'}}\frac{n_{nL}}{n_{n'L'}}\frac{\Gamma_{nL\to n''L''}}{\Gamma_{n'L'\to n''L'}}, \tag{12}$$

where ν_{nL} is the transition frequency, ε_{nL} is the detection system efficiency at the frequency of interest, $I_{nL\to n''L''}$ is the fluorescence intensity from the $nL \to n''L''$ transition. Experimentally, we can measure the cesium atom density of $6P$ state using optical absorption method, the natural radiative rates are taken from Refs. [9] and [10], k_{7D} was determined by Ref. [8], k_{9D} can be obtained from Eq. (11). By measuring the ratio n_{7F}/n_{11S} in different cesium atom densities and Eq. (9), we can obtain k_{11S}/k_{7F} and k_1, k_2. Then we also obtain k_{11S} from Eq. (10).

The experimental setup is shown in Fig. 2. Cesium metal was contained in a cylindrical Pyrex glass cell with length of 6 cm and inner diameter of 2 cm. The cell was fitted with two quartz windows and a 1-cm-long side-arm protruding from the bottom. The cell was sealed after baking and evacuating. The body of the cell was enclosed in an oven heated with resistive heater tapes. The side-arm was heated separately and was kept 30 K below the cell temperature to prevent condensation of cesium on the windows. In order to control the change in

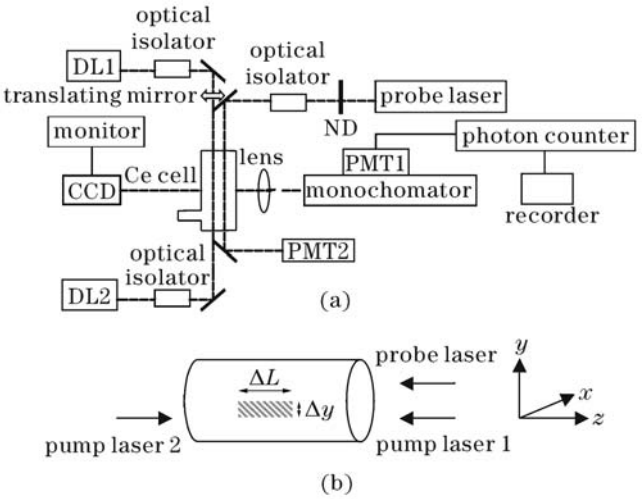

Fig. 2. (a) Experimental setup. ND: neutral density filter. (b) Cell geometry and the region from which fluorescence was detected.

transparency of the cell windows, the absorption of the white light beam at 550—650 nm was measured (not displayed in figure). The temperature of the cell was measured with thermocouples. The density of cesium atoms in the vapor phase was calculated from the vapor density formula[11]. A single-mode diode laser (DL1) was tuned to the 852.3 nm Cs($6S_{1/2} \to 6P_{3/2}$) transition. Laser power was 50 mW. The resonance fluorescence signal was observed with a charge coupled device (CCD). Another diode laser (DL2) was tuned to the Cs($6P_{3/2} \to 9S_{1/2}$) transition.

Perpendicular to the direction of the laser beam, a pair of lenses was used to image fluorescence onto the slits of 0.66-m monochromator with 1200 groove/mm grating, the volume from which fluorescence was collected was a strip with width of $\Delta y \sim 0.5$ mm and length of $\Delta L \sim 5$ mm oriented along the laser propagation (z) axis. A photomultiplier tube (PMT1) was used to detect the resolved fluorescence. The PMT signals were processed by a photon-counter and displayed on a chart recorder. The wavelength-dependent relative detection system efficiency ε was measured using a calibrated tungsten-halogen lamp.

A single-mode diode laser was used to probe the density of the atoms in the $6P_{3/2}$ level. The power of the probe laser was cut down to ~ 1 μW with a neutral density filter. We directly measured the $6P_{3/2}$ density by scanning the probe laser over the $6P_{3/2} \to 9S_{1/2}$ transition and monitoring its transmission using another photomultiplier tube (PMT2). The probe laser was stepped across the cell parallel to the pump beam using the translating mirror shown in Fig. 2. The transmitted intensity of the probe laser beam through a length L of the vapor is given by

$$I_\nu(L) = I_\nu(0)\mathrm{e}^{-k_{9S_{1/2}\leftarrow 6P_{3/2}}(\nu)L}, \tag{13}$$

for light of frequency ν, where $I_\nu(0)$ is the incident intensity and $k_{9S_{1/2}\leftarrow 6P_{3/2}}(\nu)$ is the frequency-dependent absorption coefficient. $n_{6P_{3/2}}$ is related to the integral of

$k_{9S_{1/2}\leftarrow 6P_{3/2}}(\nu)$ by

$$\int k_{9S_{1/2}\leftarrow 6P_{3/2}}(\nu)\mathrm{d}\nu = \frac{(\lambda_{9S_{1/2}\leftarrow 6P_{3/2}})^2}{8\pi}\frac{g_{9S_{1/2}}}{g_{6P_{3/2}}}n_{6P_{3/2}}\Gamma_{9S_{1/2}\leftarrow 6P_{3/2}}, \quad (14)$$

where $g_{9S_{1/2}}$ and $g_{6P_{3/2}}$ are the degeneracies of the $9S_{1/2}$ and $6P_{3/2}$ states, respectively. Thus we can extract $n_{6P_{3/2}}$ from the position dependent probe transmission scans using Eqs. (13) and (14).

In our experiment, the cell temperature is varied between 260 and 350 °C, the corresponding cesium atoms densities are $10^{16} - 10^{17}$ cm^{-3}. The fluorescence intensities of $11S \rightarrow 6P$ (574.8 nm, 557.0 nm), $7F \rightarrow 5D$ (687.2 nm, 682.7 nm), and $9D \rightarrow 6P$ (584.7 nm, 566.6 nm) are recorded in different cesium atoms densities, in the same volume and solid angle. The population ratios are obtained from Eq. (12) using the measured fluorescence intensity ratios (corrected for the detection system efficiency). Data fit with Eq. (9) and the best-fit parameters are $k_{11S}/k_{7F} = 0.75$, $k_1 = 4.0 \times 10^{-9}$ cm^3/s and $k_2 = 5.9 \times 10^{-10}$ cm^3/s.

The best-fit curve for n_{7F}/n_{11S} versus the cesium atom density is shown in Fig. 3. The values of k_1 and k_2 are combined with $\Gamma_{9D} = 1.1 \times 10^7$ s^{-1}[9] to find k_{11S}/k_{9D} in different cesium atom densities using Eq. (10). The average value of k_{11S}/k_{9D} is 0.87 (see Table 1).

At the temperature of 335 °C (the cesium atom density is 8×10^{16} cm^{-3}), the fluorescence intensities of $6P \rightarrow 6S$ (894.6 nm, 852.3 nm), $7D \rightarrow 6P$ (697.5 nm, 672.5 nm), and $9D \rightarrow 6P$ (584.7 nm, 566.6 nm) are measured. The measured values are combined with the effective radiative rates in Ref. [12] to yield the population ratios in Eq. (11). These population ratios, with the density of the atoms in the $6P_{3/2}$ state ($n_{6P} = 7.9 \times 10^{12}$ cm^{-3}) and the rate coefficient k_{7D}[8], yield the rate coefficient k_{9D}.

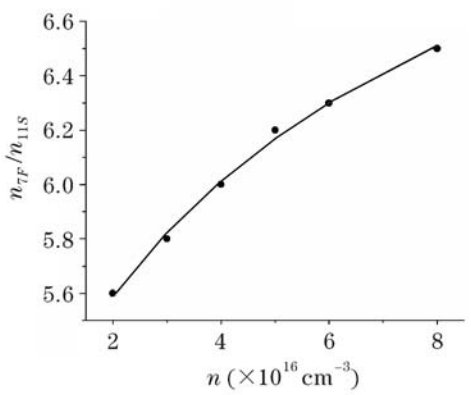

Fig. 3. Population ratio of the $7F$ to $11S$ level.

Table 1. Determination of k_{11S}/k_{9D}

n (cm^{-3})	n_{9D}/n_{11S}	n_{7F}/n_{11S}	k_{11S}/k_{9D}
2×10^{16}	1.7	5.6	0.92
3×10^{16}	2.1	5.8	0.86
4×10^{16}	2.3	6.0	0.83

Table 2. Determination of k_{nL}, $\Gamma_{6P\rightarrow 6S} = 8 \times 10^4$ s^{-1}[12], $k_{7D} = 4.4 \times 10^{-9}$ cm^3/s[8]

n_{9D}/n_{7D}	n_{6P}/n_{7D}	k_{9D} (cm^3/s)	k_{11S} (cm^3/s)	k_{7F} (cm^3/s)
0.22	5.2×10^2	8.0×10^{-10}	7.0×10^{-10}	9.3×10^{-10}

The average values of k_{11S}/k_{7F} and k_{11S}/k_{9D}, k_{11S} and k_{7F} are obtained (see Table 2).

The uncertainty density in $6P_{3/2}$ is about 25%. Fluorescence ratios probably have an uncertainty as much as 20%. The uncertainties in effective radiative rate are approximately 25%. The uncertainty in k_{7D} is about 32%[8]. Considering these various sources of statistical uncertainty, we estimate overall errors of $\sim 50\%$ in our measured energy pooling rate coefficients.

If the energy transfer process (3) between $11S$ and $7F$ is neglected, k_{nL} can be rewritten as

$$k_{nL} = 2k_{7D}^2\frac{\Gamma_{nL}}{\Gamma_{7D}^2}\frac{n_{nL}}{n_{7D}}\frac{n_{6P}}{n_{7D}}n_{6P} \quad (nL = 11S, 7F). \quad (15)$$

The calculated results are $k_{11S} = 8.6 \times 10^{-11}$ cm^3/s and $k_{7F} = 9.5 \times 10^{-10}$ cm^3/s. k_{11S} is about one order of magnitude smaller than that in Table 2 and k_{7F} has a little change. It is shown that the energy transfer process between $11S$ and $7F$ has a considerable influence on the determination of k_{11S}. Our value for $5D + 5D \rightarrow 6S + 7F$ rate coefficient is in agreement, within error bar, with the value obtained under different experimental conditions[13].

This work was supported by the National Science Foundation of China under Grant No. 10264004. Y. Shen is the author to whom the correspondence should be address, his e-mail address is shenyifan01@xju.edu.cn.

References

1. M. Allegrini, G. Alzetta, A. Kopystynska, L. Moi, and G. Orriols, Opt. Commun. **19,** 96 (1976).
2. M. Allegrini, C. Gabbanini, L. Moi, and R. Colle, Phys. Rev. A **32,** 2068 (1985).
3. Y.-F. Shen, K. Dai, B.-X. Mu, S.-Y. Wang, and X.-H. Cui, Chin. Phys. Lett. **22,** 2805 (2005).
4. S. Gozzini, S. A. Abdullah, M. Allegrini, A. Cremoncini, and L. Moi, Opt. Commun. **63,** 97 (1987).
5. D. Azinović, I. Labazan, S. Milošević, and G. Pichler, Opt. Commun. **183,** 425 (2000).
6. R. K. Namiotka, J. Huennekens, and M. Allegrini, Phys. Rev. A **56,** 514 (1997).
7. J. Huennekens, Z. Wu, and T. G. Walker, Phys. Rev. A **31,** 196 (1985).
8. Y.-F. Shen and W.-X. Li, Acta Phys. Sin. (in Chinese) **42,** 1766 (1993).
9. C. E. Theodosiou, Phys. Rev. A **30,** 2881 (1984).
10. B. Warner, Mon. Not. R. Astr. Soc. **139,** 115 (1968).
11. C. Vadla, V. Horvatic, and K. Niemax, Spectrochimica Acta Part B **58,** 1235 (2003).
12. B. Keramati, M. Masters, and J. Huennekens, Phys. Rev. A **38,** 4518 (1988).
13. C. Vadla, K. Niemax, and J. Brust, Zeitschrift Für Physik D **37,** 241 (1996).